Grazing-incidence antireflection films. II. Alternate techniques and general multilayer theory

J. P. Hannon, N. V. Hung, and G. T. Trammell
Physics Department, Rice University, Houston, Texas 77251

E. Gerdau, M. Mueller, R. Rüffer, and H. Winkler
Institut für Experimentalphysik, Universität Hamburg, Hamburg, Germany

(Received 9 May 1984)

In this second of two papers on nonresonant grazing-incidence antireflection films, we examine alternate techniques for achieving high-efficiency antireflection films for suppressing hard-x-ray reflections: half-wave films, layered ultrathin films, general multilayer techniques, and tapered impedance films.

I. INTRODUCTION

In the preceding paper I,[1] we discussed the possibility of grazing-incidence antireflection films for creating high-efficiency antireflection coatings for near-grazing-incidence reflection of hard x rays and γ rays. Our motivation is the possible application of producing "ultranarrow" bandpass filters for synchrotron radiation with frequency widths $\approx 10^{-8}$–10^{-6} eV, giving a unique high-resolution, long-coherence-length x-ray source for probing inelastic excitations and opening new possibilities in x-ray interferometry. In paper I we developed the general theory and examined the simplest ideas for achieving antireflection films—impedance-matched quarter-wave films and damping-stabilized solutions—which can both be obtained by coating a high-density mirror with a single lower-density film.

In this paper we discuss a number of alternate techniques for strongly suppressing x-ray reflections: half-wave films, layered ultrathin films, general multilayer techniques, and tapered impedance films. Sections II and III are direct applications of the development given in paper I,[1] and Sec. IV gives a general multilayer theory for grazing-incidence antireflection (GIAR) films.

II. $\lambda/2$ FILMS

If the electron density of the film is *higher* than that of the backing so that now $\phi_{c1} > \phi_{c2}$, then a true antireflection coating is impossible: Due to the backing, the electron-density change at the 0-1 interface is necessarily greater than at the 1-2 interface, and the impedance-match condition $r_{01} = r_{12}\exp(-2g_1'' l_1)$ can no longer be satisfied. Nevertheless, destructive interference still occurs, now at a half-wave condition. Because of the lack of impedance match, the reductions are rather modest but, for some purposes, these may be sufficient.

As a typical example, we consider an Fe film on Si, reflecting 14.4-keV radiation ($\phi_{c1} = 3.8$ mrad, $\phi_{c2} = 2.1$ mrad). The reflection amplitude is given by the general expression, Eq. (9) or (17) of paper I. Figure 1 gives the rocking curves for the interface reflection amplitudes r_{01} and $r_{12}\exp(-2g_1'' l_1)$ and for the corresponding phases ϕ_{01} and ϕ_{12}.

The behavior of the reflection amplitudes has important modifications from the low-density-film case (Fig. 6 of paper I) because now $\phi_{c1} > \phi_{c2}$: As before, r_{01} has near-total reflection for $\phi < \phi_{c1}$, while r_{12} has a near-total reflection region for $\phi_{c2} \le \phi \le \phi_{c1}$. However, when damping effects are included, the lower interface reflection $r_{12}\exp(-2g_1'' l_1)$ peaks only near ϕ_{c1} because there is strong primary extinction for $\phi < \phi_{c1}$, the total reflection region for the upper medium. Because $\phi_{c2} < \phi_{c1}$, $r_{12}\exp(-2g_1'' l_1)$ is everywhere less than r_{01} and there can be no impedance match. For interference, the region of interest is $\phi > \phi_{c1}$, where deep penetration into film 1 occurs, and in this region r_{01} and $r_{12}\exp(-2g_1'' l_1)$ slope together, with the difference remaining fairly small, $\approx \phi_{c2}^2/4\phi^2$.

The rocking curves for the phases ϕ_{01} and ϕ_{12} of the interface reflections are shown in Fig. 1(b). As for the low-density case, ϕ_{01} increases rapidly from $-\pi \to 0$ as $\phi \propto 0 \to \phi_{c1}$, but now, ϕ_{12} increases from $0 \to \pi$ as $\phi \propto \phi_{c2} \to \phi_{c1}$. The phases are constant outside of these regions, and in the interference region $\phi > \phi_{c1}$, the phase difference is $\phi_{01} - \phi_{12} \simeq -\pi$, corresponding to the expected opposite signs of R_{01} and R_{12}.

The condition for destructive interference is again given by Eq. (21) of paper I, but now, $\phi_{01} - \phi_{12} \simeq -\pi$ and the required film thickness is a "half-wave film,"

$$l_1^{(2n+1)\pi}(\phi) \simeq n\lambda/2(\phi^2 - \phi_{c1}^2)^{1/2} . \tag{1}$$

A simple estimate can be given for the strength of the impedance mismatch which occurs at the interference minima: Conceptually taking a small gap $\Delta l \to 0$ between film 1 and medium 2, then, in the single scattering approximation, the total reflection will be a superposition of three vacuum-interface reflections, giving

$$R_{\min} \simeq r_{01}(1 - e^{-2g_1'' l_1}) + r_{02} e^{-2g_1'' l_1} . \tag{2}$$

The first contribution gives the reflection from a free film at the $\lambda/2$ condition, and here the impedance mismatch is due entirely to photoabsorption. The second contribution

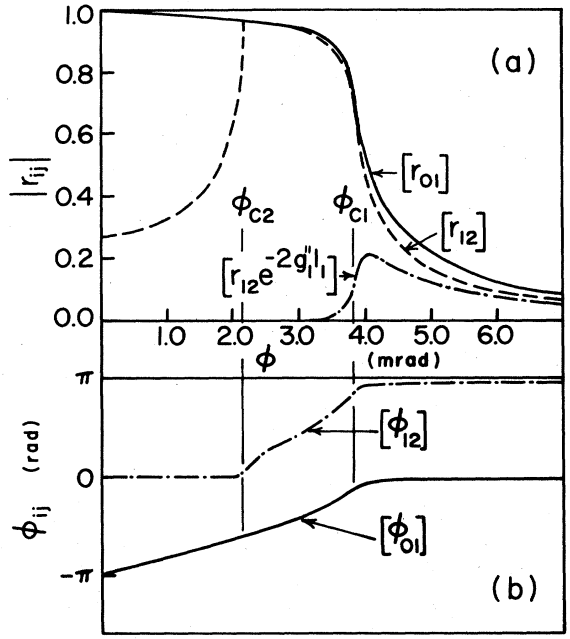

FIG. 1. (a) Interface reflection amplitudes, and (b) phases vs the incidence angle ϕ for 185-Å Fe film on Si, reflecting 14.4-keV radiation.

is the vacuum-substrate reflection, with a photoabsorption reduction for propagation through film 1. Both contributions are positive and add constructively to increase the total reflection.

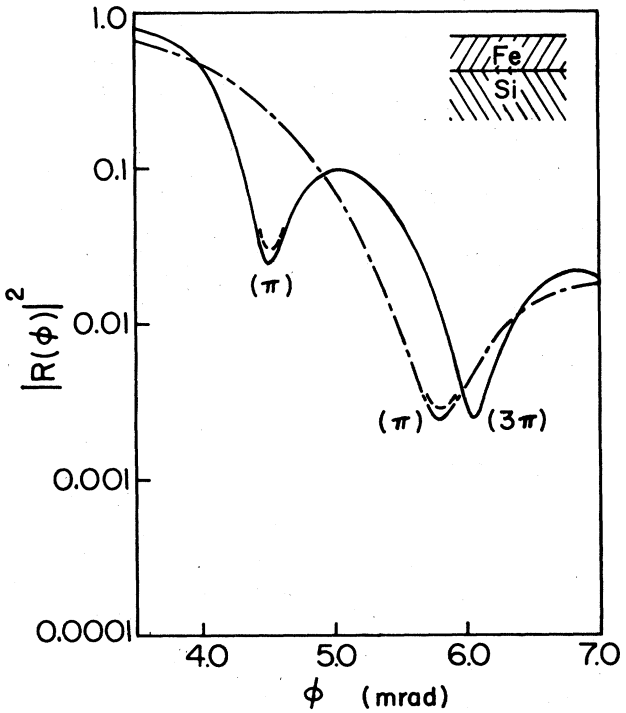

FIG. 2. Rocking curves $|R|^2$ vs ϕ for 185-Å Fe on Si (solid curve) and 100-Å Fe on Si (dashed curve), reflecting 14.4-keV radiation.

From this estimate it is clear that the reflection can be minimized by taking the lowest-density substrate possible to reduce r_{02} and by taking a thinner film l_1 and a larger incidence angle ϕ to reduce the path length in film 1 and the photoabsorption factor $[1-\exp(-2g_1''l_1)]$. The increased ϕ also acts to further reduce r_{02}.

As an example, for a 185-Å Fe film on Si and 14.4-keV radiation, the first $\lambda/2$ minimum occurs for $\phi_0=4.5$ mrad and Eq. (2) gives a reflectivity $|R|^2\simeq 0.02$ in a region where normally $|R|^2\simeq 0.10$. On the other hand, for a 100-Å film, $\phi_0=5.7$ mrad and $|R|^2\simeq 2\times 10^{-3}$ in a region where normally $|R|^2_{\mathrm{Fe}}\simeq 0.01$. In both cases the reduction factor $|R|^2/|R|^2_{\mathrm{Fe}}\approx\frac{1}{5}$. These estimates are in good agreement with the minima of the exact rocking curves shown in Fig. 2.

There is a practical advantage to $\lambda/2$ films: In contrast to $\lambda/4$-GIAR films, no careful matching of densities and thicknesses is required since any thickness high-density film on a low-density backing will have a series of interference minima for $\phi>\phi_{c1}$. Although the reduction factors are not very pronounced, for some applications they may be sufficient.

III. ULTRATHIN FILMS

Our primary interest in GIAR films is for resonant γ-ray optics. For the ^{57}Fe 14.4-keV transition, the resonance scattering is an order of magnitude greater than the nonresonance electronic scattering. Because of this difference in scattering strengths, another technique for reducing the electronic scattering is to use an "ultrathin" film $\approx$10—20 Å, which is "thin" for the electronic scattering but still "thick" for the resonant nuclear scattering.

A. Single ultrathin film on low-density backing

For a single ultrathin film on a low-density backing, the reflected wave amplitude is still given by Eq. (9) or (17) of paper I. On a low-density backing, $R_{12}\simeq -R_{01}$ and there is a strong reduction in scattering if the film is sufficiently thin, so that the phase factor $\exp(i2g_1l_1)\simeq 1$.

The condition for an ultrathin (UT) film is then

$$l_1 < l_{\mathrm{UT}}(\phi)=(2|g_1|)^{-1} =\lambda/\{2[(\phi^2-\phi_{c1}^2)^2+(\lambda/l_A)^2]^{1/4}\}\ . \quad (3)$$

The most favorable case is for $\phi\approx\phi_{c1}$, where the refracted wave is nearly parallel to the surface. Figure 3 gives $l_{\mathrm{UT}}(\phi)$ for the ^{57}Fe case which has a peak value $\approx$81 Å at $\phi=\phi_{c1}$.

For films with $l_1\ll l_{\mathrm{UT}}(\phi)$, there is little extinction or phase change across the film. All atoms then reflect in phase into the reflection channel and the reflected amplitude increases with increasing thickness for thicknesses up to $\approx l_{\mathrm{UT}}$. Thus, for $l_1\ll l_{\mathrm{UT}}(\phi)$, the reflection amplitude is reduced from r_{01} approximately by a factor $l_1/l_{\mathrm{UT}}(\phi)$.

More exactly, if $l_1<l_{\mathrm{UT}}(\phi)$, the reflection amplitude, Eq. (9) of paper I reduces to

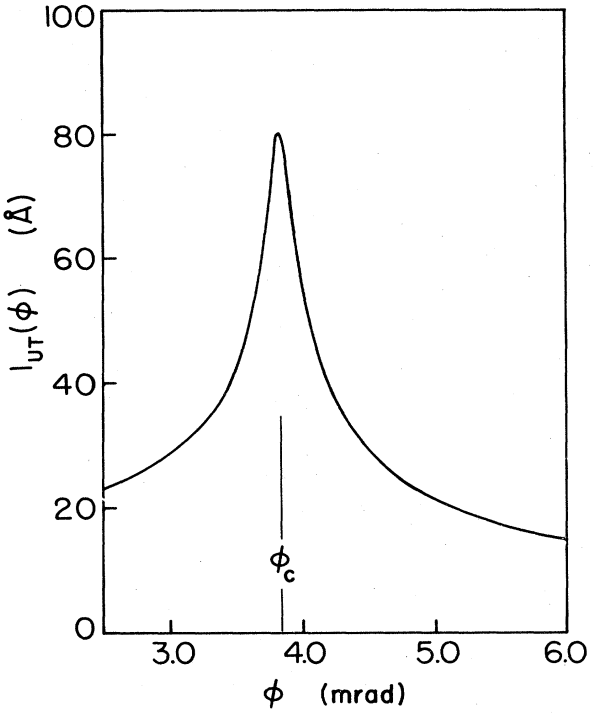

FIG. 3. Ultrathin-film limiting thickness $l_{UT}(\phi)$ vs ϕ for Fe, reflecting 14.4-keV radiation.

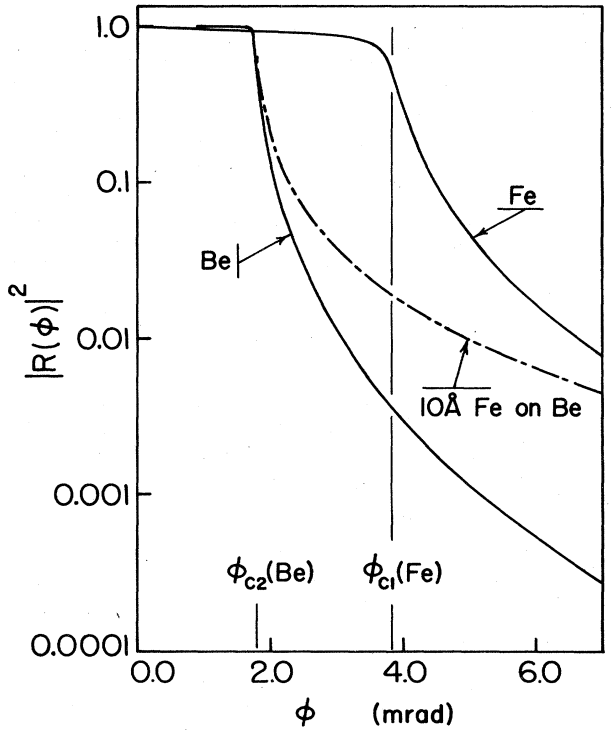

FIG. 4. Rocking curve $|R|^2$ vs ϕ for a single ultrathin film of 10-Å Fe on Be, reflecting 14.4-keV radiation (dashed curve). The solid curves give the reflectivities for pure Fe and pure Be.

$$R(\phi)\simeq iF(l_1)+R_{02}\ , \tag{4}$$

where

$$F(l_1)=n\lambda l_1 f_e/\phi=-(\pi\phi_c^2 l_1/\lambda\phi)(1-i\lambda/\phi_c^2 l_A)\ . \tag{5}$$

The first contribution to R, $iF(l_1)$, gives the scattering from a free UT film, while the second contribution R_{02} gives the scattering from the uncoated backing.

Now, $iF(l_1)$ is just the usual Born approximation for scattering from a "single plane" (see Appendix A of paper I). The scattering is necessarily 90° out of phase with the primary wave [so that in the forward direction the imaginary contribution to $F(l_1)$, which is due to the total absorption cross section, will give a wave 180° out of phase with the primary, leading to extinction]. Because of the 90° phase shift and because $F(l_1)$ and R_{02} are both essentially real (in the region $\phi>\phi_{c2}$), there is little interference between the UT film and substrate reflections, and $|R|^2\simeq F(l_1)^2+R_{02}^2$. To minimize the backing contribution, the substrate should be taken with the lowest density possible. As a specific example, consider 10 Å of Fe on a Be backing reflecting 14.4-keV radiation. Then for $\phi\approx\phi_{c1}$, $F(l_1)^2\simeq 0.02$ and $R_{02}\simeq 0.003$, giving a reflection $|R|^2\simeq 0.02$ in a region of near-total reflection from a pure Fe mirror.

Figure 4 gives the exact rocking curve $|R(\phi)|^2$ for a 10-Å Fe film on Be, and also for $|R_{01}(\phi)|^2$ (pure Fe) and $|R_{02}(\phi)|^2$ (pure Be). In the region $\phi\approx\phi_{c1}$ we see that $|R|^2$ is reduced from $|R_{01}|^2$ by a factor $\simeq\frac{1}{30}$, which is a considerably stronger reduction factor than for a $\lambda/2$ film.

B. UT-film interference techniques

Although a fairly strong reduction can be achieved with a single ultrathin film, the reflectivity is still $|R|^2\gtrsim 10^{-2}$, and for applications such as synchrotron filtering, we would like $|R|^2\lesssim 10^{-3}$. To achieve such a strong reduction it is necessary to use interference.

One simple method is to use two UT layers l_1 and l_3, separated by a low-density film l_2 and coated on a low-density backing, as indicated in Fig. 5(a). In the UT limit, the multilayer reflection amplitude is approximately

$$R(\phi)\simeq iF(l_1)+R_{02}+iF(l_3)e^{i2g_2l_2}+R_{24}e^{i2g_2l_2}\ . \tag{6}$$

Here, $iF(l_1)$ and $iF(l_3)$ are the scattering contributions from the two (free) UT films, R_{02} is the reflection from a vacuum-medium-2 interface, and R_{24} is the reflection from a medium-2—medium-4 interface. As noted before, the UT limit holds best for $\phi\simeq\phi_{c1}$ $(=\phi_{c3})$.

Because the UT reflections are 90° out of phase with the 0-2,2-4 interface reflections, there is *separate* interference between the two UT reflections and between the two interface reflections. If medium 4 is taken at higher density than medium 2, then both R_{24} and $R_{02}>0$, and there will be simultaneous destructive interference between the two UT reflections and between the two interface reflections when a quarter-wave condition holds for l_2 so that $\exp(i2g_2l_2)=-1$. In principle, we could take the density of medium 2, such that an impedance match would also occur at this angle, giving $R_{02}\approx R_{24}$. However, it is un-

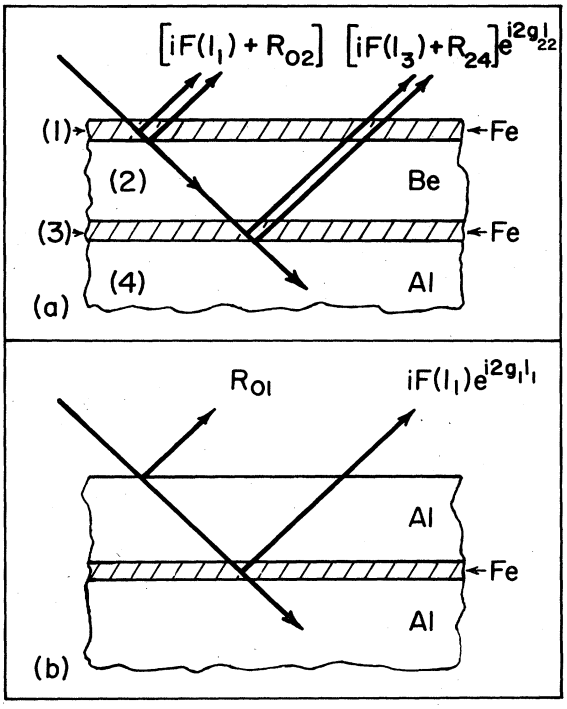

FIG. 5. Geometry for (a) two-layered ultrathin films, and (b) for a single ultrathin film coated with a $3\lambda/8$ film.

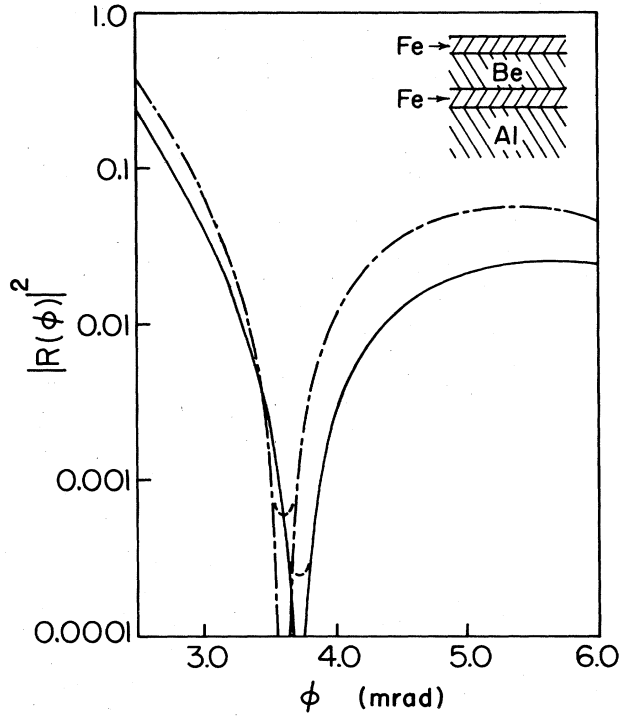

FIG. 6. Rocking curves for layered ultrathin films (10-Å Fe—64-Å Be—12-Å Fe-Al) (solid curve) and (15-Å Fe—64-Å Be—17-Å Fe-Al) (dashed curve), reflecting 14.4-keV radiation.

necessary to strive for exact cancellations here because all amplitudes are already small, and with only partial cancellations, it should still be easy to achieve $|R|^2 \lesssim 10^{-3}$. Thus, in practice, it should suffice to take media 2 and 4 as any two low-density media, with critical angles $\phi_{c2} < \phi_{c4} \ll \phi_{c1}$ so that R_{02} and R_{24} are small for $\phi \approx \phi_{c1}$ (where the UT limit holds best) and with $l_2 \simeq \lambda/4(\phi_{c1}^2 - \phi_{c2}^2)^{1/2}$ so that a $\lambda/4$ condition holds for $\phi \approx \phi_{c1}$. Also, the UT film 2 needs to be somewhat thicker than the UT film 1 to offset the small extinction effects in films 1 and 2.

As an example, in Fig. 6 we give the exact rocking curve $|R(\phi)|^2$ for a 10-Å Fe—64-Å Be—12-Å Fe-Al multilayer which has a very pronounced minimum $|R|^2 < 10^{-4}$ for $\phi \simeq 3.7$ mrad. The dashed curve in Fig. 18 gives the corresponding results for a 15-Å Fe—64-Å Be—17-Å Fe-Al multilayer which also has a pronounced minimum, but shifted to $\phi \simeq 3.6$ mrad by the thicker films. An exact solution procedure to determine the optimum l_1, l_2, and l_3 is given in the following section. Such UT-GIAR films should be capable of giving as strong a suppression of x-ray reflection as $\lambda/4$-GIAR films, and in practice it may be easier to achieve strong suppression with UT-GIAR films because it is unnecessary to try to impedance match at the $\lambda/4$ condition.

An alternate UT-film interference technique is a $3\lambda/8$-coated UT film indicated in Fig. 5(b): An UT film of Fe is coated on a low-density mirror, say, Al and then a film of the mirror material (Al) is coated on top. In the UT-film limit, the reflection amplitude is then approximately

$$R \simeq R_{01} + e^{i2g_1l_1} iF(l_2) . \tag{7}$$

For $\phi \simeq \phi_{c2}$(Fe), R_{01} is small and positive and $F(l_2)$, as given by Eq. (5), is negative. To get destructive interference the thickness of film 1 should then be taken so that $2g_1l_1 = 3\pi/2$, which requires l_1 to be a $3\lambda/8$ coated film,

$$l_1 = 3\lambda/8(\phi^2 - \phi_{c1}^2)^{1/2} . \tag{8}$$

For optimum suppression, the thickness of the UT film should be chosen to give an impedance match, i.e., $-F(l_2) = R_{01}$, which requires

$$l_2 \simeq \lambda r_{01}/\pi\phi_{c2} . \tag{9}$$

With Al ($\phi_c = 2.27$ mrad) as the backing and a $3\lambda/8$ coating, then at $\phi = \phi_{c2} = 3.84$ mrad these estimates give $l_1 = 104$ Å (Al) and $l_2 = 8$ Å (Fe). An exact procedure for determining the optimum l_1, l_2 is given in the following section.

IV. MULTILAYER GIAR FILMS

The layered ultrathin GIAR films discussed above are examples of multilayer techniques. In the optical and infrared regions, multilayer techniques are widely used to produce more effective antireflection filters and to greatly extend the choice of suitable materials. There is extensive literature on such multilayer techniques,[2–4] all of which can be carried over directly to GIAR films. However, the effectiveness of many of these techniques is severely limited by strong photoabsorption.

For GIAR films there are three main advantages to multilayer coatings: First, with additional layers, it is

possible to reduce the density change in adjacent films, thereby reducing the amplitude of the interface reflections. Just as for the UT-GIAR films, interference is then between small amplitudes, which improves the effectiveness of the filter. Secondly, with more than one layer, it is possible to produce a secondary minimum close to the primary minimum, with the result that there is a greatly increased region of strong suppression. (In contrast, for a single film, the minima are regularly spaced at 2π intervals of the phase $\psi_1=2g_1l_1$, with intermediate regions of strong constructive interference.) The most important advantage is that with more than one layer, the thicknesses of the additional layers are new variable parameters and it is possible to achieve impedance match and phase cancellation by adjusting the film thicknesses. Such "thickness tuning" makes it possible to arbitrarily specify the incidence angle ϕ_0, which is not possible for single-layer GIAR films and greatly extends the choice of film materials.

A. Fractional wavelength multilayer films

In the optical region, there are a number of filter techniques utilizing fractional wavelength coatings—primarily various combinations of half- and quarter-wave coatings. In these systems impedance matching is made by a proper choice of the indices of refraction of the various layers, i.e., by "index-of-refraction tuning." The advantage here is that for a nonabsorbing dielectric film, the characteristic matrix $\tilde{\mathscr{M}}$ (see Appendix B of paper I) greatly simplifies for a quarter- or half-wave thickness and there is a consequent simplification of the analysis for a series of such films. However, in the presence of strong absorption, there is no special simplification at half- or quarter-wavelengths and, hence, for GIAR films there is no particular advantage in using fractional wavelength films. Because of the limited usefulness, we will not give a complete account of fractional wavelength GIAR films, but we mention two cases of interest.

1. *Quarter-coated λ/2 film*

As discussed in Sec. II, it is impossible to achieve an impedance match in a single half-wave film: the amplitude of the lower interface reflection is reduced by the substrate and by strong photoabsorption in transversing the film, leaving the wave too weak to cancel the upper surface reflection. However, the upper surface reflection can be reduced by coating the λ/2 film with a low-density quarter-wave coat; for example, coating a 185-Å Fe film, which is a λ/2 film for 14.4-keV radiation at $\phi_0=4.5$ mrad, with a 55-Å Al film, which is a λ/4 film at ϕ_0. The addition of Al reduces the upper Fe interface reflection, and because of the λ/4 condition, the Al-Fe reflection is further reduced by destructive interference with the reflection from the upper Al surface.

In the single scattering approximation, the total reflection amplitude at ϕ_0 is then given approximately by

$$R(\phi_0)\simeq 2R_{01}-R_{02}^{\dagger}\ , \tag{10}$$

where R_{01} is the reflection amplitude for a single (vacuum-) Al surface and $R_{02}^{\dagger}$ is the total reflection amplitude for the λ/2 film plus substrate, given approximately by Eq. (2). For an optimum coating, the quarter-wave film should be chosen so that

$$R_{01}\gtrsim\tfrac{1}{2}R_{02}^{\dagger}\ . \tag{11}$$

The main problems are finding a material of proper electron density, and the increased difficulty of achieving precise thickness control for two films rather than one.

For the 185-Å Fe film on Si, $R_{02}^{\dagger}\simeq 0.16$ at $\phi_0=4.5$ mrad, while for Al, $2R_{01}(\phi_0)\simeq 0.14$, a little low for an optimum coating. Nevertheless, as shown in Fig. 7, the minimum reflectivity is reduced to $|R|^2\approx 7\times10^{-4}$ or $\langle|R|^2\rangle\approx 4\times10^{-3}$ when averaged over an angular spread of $\Delta\phi\approx 0.2$ mrad, which is a significant improvement over the response for the uncoated film shown by the dashed curve.

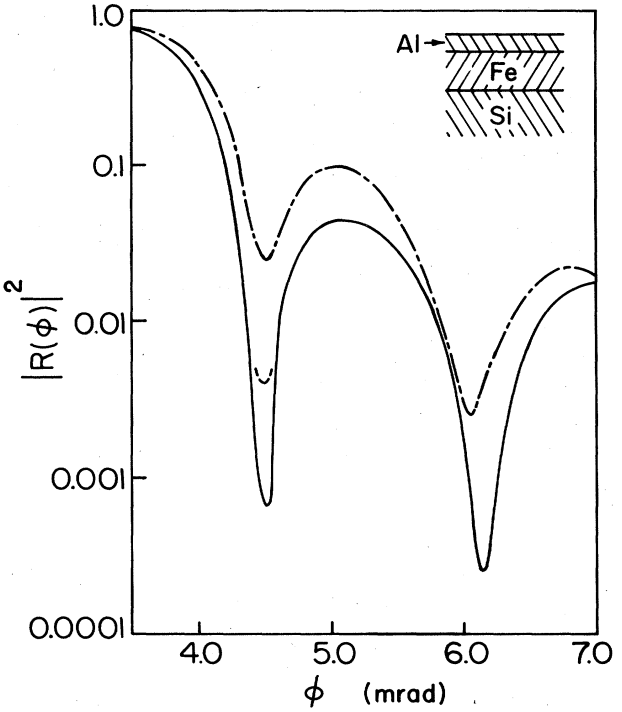

FIG. 7. Rocking curve for λ/2 film of Fe ($l_2=185$ Å) coated with a λ/4 film of Al ($l_1=55$ Å) with minimum at $\phi_0=4.5$ mrad. The dashed curve gives the uncoated response.

2. *Impedance-matched λ/2N-GIAR film*

Another multilayer technique, which illustrates several of the general features mentioned above but appears of limited practical use, is to coat a high-density mirror with a "staircase" series of $N-1$ films, each of optical path $\lambda/2N$ and with increasing electron density, to give equal reflection amplitudes at each interface, i.e., $R_{n,n+1}=R_{01}$ for $n=0,1,\ldots,N-1$.

For GIAR films, the impedance-match condition reduces to $\beta_{n+1}/\beta_n=\beta_N^{1/N}$ or $\beta_n=\beta_N^{n/N}$, and the ampliude of each interface reflection is then

$$R_{n,n+1}=R_{01}=\frac{1-\beta_N^{1/N}}{1+\beta_N^{1/N}}\ , \tag{12}$$

which is strongly reduced from the uncoated mirror reflection amplitude of $(1-\beta_N)/(1+\beta_N)$. In the single scattering approximation the total scattering amplitude for the series is then

$$R=\sum_{n=0}^{N-1} R_{n,n+1}\exp\left[i\sum_{m=0}^{n}\psi_m\right]\ , \tag{13}$$

where $\psi_m=2g_m l_m=4\pi\phi\beta_m l_m/\lambda$ is the phase for transversal through the mth film.

The general phasor addition diagram for graphically summing the series of Eq. (13) is shown in Fig. 8(a). Here, $N=3$, and it is assumed $R_{n,n+1}$ is real and positive, i.e., increasing density, $\phi>\phi_c$, and $\sigma_e=0$.

With impedance-matched amplitudes $r_{n,n+1}$ the condition for *destructive interference* is then that all $\psi_m=2\pi/N$ (or an integral multiple $\neq N$), which closes the phasor diagram as shown in Fig. 8(b). Each film will then be a "$\lambda/2N$ film," with the thickness of the nth film being

$$l_n=\lambda/[2N\phi_0\beta_n(\phi_0)]\ . \tag{14}$$

The chosen angle ϕ_0 is then the primary interference minimum. However, the ψ_m are to first approximation linear in ϕ and, hence, as ϕ increases there will be secondary minima whenever all ψ_m are approximately integral multiples of $2\pi/N$.

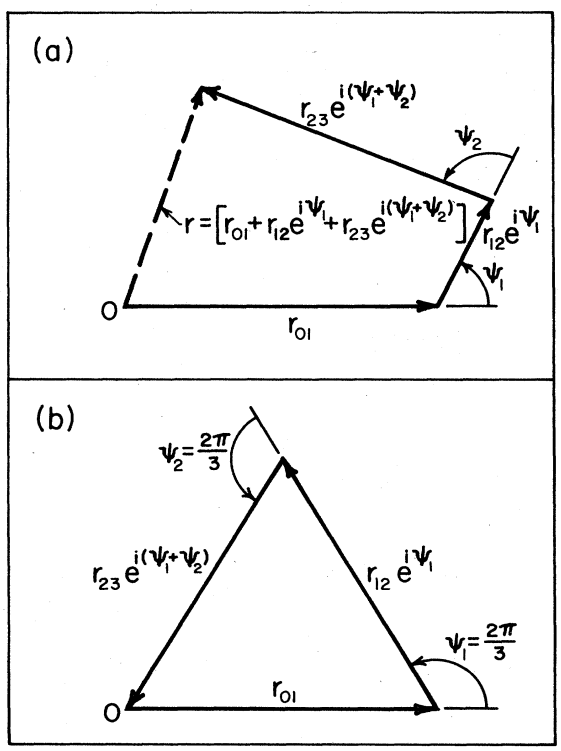

FIG. 8. (a) General phasor-addition diagram for three interface reflection amplitudes. (b) Closed phasor diagram for reflection from a mirror coated with two-impedance-matched ($r_{01}=r_{12}=r_{23}$) $\lambda/6$ films ($\psi_1=\psi_2=2\pi/3$).

An important point is that in the regions between the interference minima, the phasors are no longer perfectly constructive. This is in contrast to the single-film case which only involves two phasors R_{01} and $R_{12}\exp(i\psi_1)$ which necessarily add constructively between any two minima. Hence, for the multilayer case, the intermediate maxima tend to be less pronounced. A basic problem here of course is finding a series of materials of proper electron density to satisfy the impedance-match condition and, in practice, the condition can only be approximately satisfied.

B. Thickness-tuned multilayer GIAR films

A much more powerful technique, and the main advantage of multilayer GIAR films, is the use of "thickness tuning," treating the film thicknesses $l_1,l_2,\ldots$ as parameters which can be adjusted to achieve both impedance match and phase cancellation. This is a distinct advantage over index-of-refraction tuning because, in contrast to electron densities which are fixed, film thicknesses can be varied continuously.

1. *Two films*

For a mirror coated with two films, the scattering amplitude in the single scattering approximation is

$$R=R_{01}+R_{12}e^{i\psi_1}+R_{23}e^{i(\psi_1+\psi_2)}\ , \tag{15}$$

where as before, $\psi_j=\psi_j'+i\psi_j''=2g_j l_j=4\pi\phi\beta_j l_j/\lambda$ is the complex phase shift for transversal through the jth film, and $R_{n,n+1}=(\beta_n-\beta_{n+1})/(\beta_n+\beta_{n+1})$ is the reflection amplitude at the $n,n+1$ interface. If the film materials are chosen such that the combined magnitude of any two reflections exceeds that of the remaining surface, i.e., if

$$r_{ij}<r_{kl}+r_{mn}\ , \tag{16}$$

then complete destructive interference can be achieved with the proper choice of the film thicknesses l_1 and l_2.

A simple graphical solution commonly used in the optical theory[2] is given in Fig. 9 for the particular case of an Fe mirror coated with Sn (film 2) and Se (film 1). We are free to specify any ϕ_0, as long as the reflection amplitudes satisfy the criteria equation (16). To be specific, we take $\phi_0=4.5$ mrad, in which case $r_{01}=0.130$, $r_{12}=0.091$, and $r_{23}=0.103$ (all in the limit $\sigma_e=0$). In Fig. 10(a) the circle C_1 of radius r_{12} is centered at the tip P_1 of the R_{01} vector, the circle C_2 of radius r_{23} is centered at the origin P_0, and the intersections P_2,P_2' determine the two possible solutions for completing the phasor diagram to give exact cancellation. For the solution P_2 of Fig. 9(b), $\psi_1=2.24$ rad and $\psi_2=1.70$ rad, which determines the thicknesses to be $l_1=44$ Å (Se) and $l_2=40$ Å (Sn). For the second solution P_2' of Fig. 10(c), the film thicknesses are $l_1=80$ Å and $l_2=109$ Å.

In this example, all $R_{n,n+1}$ are real and positive, which implies increasing electron density, $\phi>\phi_{c3}$, and $\sigma_e=0$. The graphical solution technique is easily modified to allow for negative $R_{n,n+1}$ or more generally complex amplitudes, but it is still necessary to require that the phases ψ_1

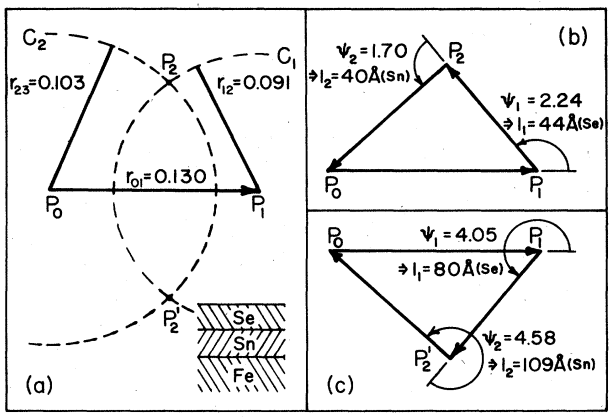

FIG. 9. Graphical solution for l_1(Se) and l_2(Sn) to give two-film antireflection coat on Fe mirror to suppress the reflection of 14.4-keV radiation incident at $\phi_0=4.5$ mrad.

and ψ_2 be purely real, which is equivalent to the restriction $\phi>\phi_c$ and $\sigma_e=0$. Furthermore, the graphical solution is a single scattering approximation which ignores multiple reflections.

However, it is easy to give a completely general exact solution which takes into account multiple scattering and photoabsorption and which can be applied to any ϕ region, including $\phi<\phi_c$. This procedure is a direct modification of the general single-film solution given in paper I: For a mirror coated with two films, the exact reflection amplitude is

$$R=\frac{R_{01}+R_{12}^{\dagger}(l_2)e^{i2g_1l_1}}{1+R_{01}R_{12}^{\dagger}e^{i2g_1l_1}}=\frac{r_{01}e^{i\phi_{01}}+r_{12}^{\dagger}(l_2)e^{-2g_1''l_1}e^{i(\phi_{12}^{\dagger}(l_2)+2g_1'l_1)}}{1+R_{01}R_{12}^{\dagger}e^{i2g_1l_1}}\ , \tag{17}$$

where $R_{12}^{\dagger}(l_2)$ is the total reflection amplitude of film 2 plus substrate reflecting into medium 1,

$$R_{12}^{\dagger}(l_2)=\frac{R_{12}+R_{23}e^{i2g_2l_2}}{1+R_{12}R_{23}e^{i2g_1l_2}}\equiv r_{12}^{\dagger}(l_2)e^{i\phi_{12}^{\dagger}(l_2)}\ . \tag{18}$$

We have also introduced the notation for the amplitudes and phases of the individual interface reflection amplitudes as in Eq. (18) of paper I, $R_{ij}=r_{ij}\exp(i\phi_{ij})$. Now, $R_{12}^{\dagger}(l_2)$ is an explicit function of l_2, so the amplitude and phase of the combined reflection can be "tuned" by varying the thickness l_2. From Eq. (17), the general *impedance-match* condition is then

$$r_{01}=r_{12}^{\dagger}(l_2)e^{-2g_1''l_1}\ . \tag{19}$$

Just as in Eq. (19) of paper I, this can be viewed as an equation for $l_1^{(=)}(l_2)$, the thickness film 1 must be taken to give an impedance match,

$$l_1^{(=)}(l_2)=\frac{\ln(r_{12}^{\dagger}(l_2)/r_{01})}{2g_1''}\ . \tag{20}$$

As a function of l_2, $r_{12}^{\dagger}(l_2)$ and, hence, $l_1^{(=)}(l_2)$ are oscillatory but slowly damped to a constant value in the limit of very large l_2. Since $|r_{12}-r_{23}|<r_{01}<[r_{12}+r_{23}]$, then $l_1^{(=)}(l_2)$ oscillates positive to negative.

The condition for *destructive interference is*

$$\exp\{i[2g_1'l_1+\phi_{12}^{\dagger}(l_2)-\phi_{01}]\}=-1\ , \tag{21}$$

which requires the relative phase to be an odd multiple of π. For a given l_2, the thickness of film 1 necessary to give a $(2n+1)\pi$ relative phase must then be

$$l_1^{(2n+1)\pi}(l_2)=\frac{(2n+1)\pi-\phi_{12}^{\dagger}(l_2)+\phi_{01}}{2g_1'}\ . \tag{22}$$

If $r_{12}<r_{23}$, then $\phi_{12}^{\dagger}(l_2)$ monotonically increases with l_2, as shown by the phasor diagram, Fig. 10(a), and in this case, $l_1^{(2n+1)\pi}$ decreases monotonically to zero. On the other hand, if $r_{12}>r_{23}$, then $\phi_{12}^{\dagger}(l_2)$ and, hence, $l_1^{(2n+1)\pi}(l_2)$ is an oscillatory function of l_2, as indicated in Fig. 10(b).

The necessary thicknesses l_1,l_2 for *antireflection coatings* are then determined by the intersections of the $l_1^{(=)}(l_2)$ curves for impedance match with the $l_1^{(2n+1)\pi}(l_2)$ curves for destructive interference.

In Fig. 11 we give $l_1^{(=)}$, $l_1^{\pi}(l_2)$, and $l_1^{3\pi}(l_2)$ for a Fe mirror coated with Sn (film 2) and Se (film 1), with ϕ_0 chosen as 4.5 mrad. The intersections P_2,P_2' give film thickness l_1,l_2 close to the phasor diagram solutions but shifted somewhat due to the effects of multiple reflections and photoabsorption.

The Fe mirror should then be coated with $l_1=44$ Å of

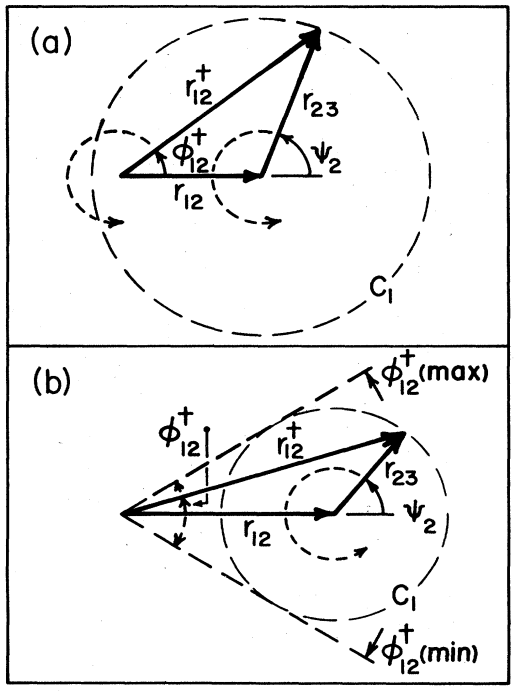

FIG. 10. Variation of $\phi_{12}^{\dagger}$ vs ψ_2 $(=2g_2l_2)$ for (a) $r_{23}>r_{12}$ and (b) $r_{23}<r_{12}$.

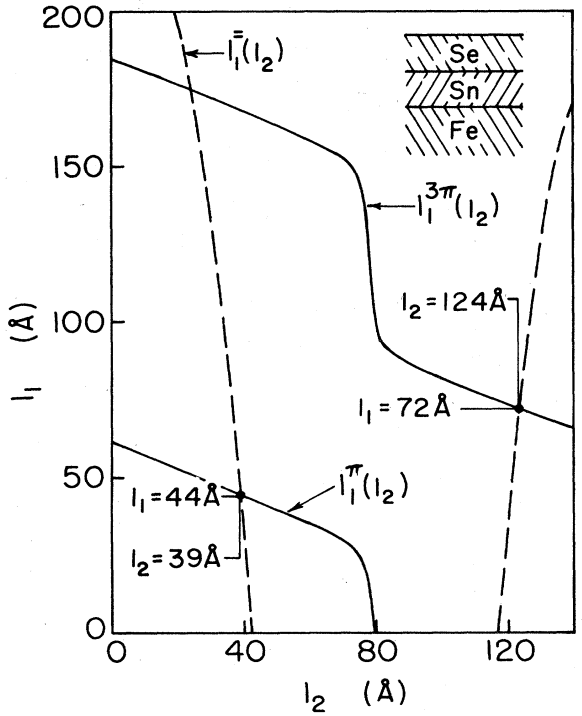

FIG. 11. $l_1^{(=)}(l_2)$, $l_1^{\pi}(l_2)$, and $l_1^{3\pi}(l_2)$ for Fe mirror coated with Sn (film 2) and Se (film 1), with ϕ_0 chosen as 4.5 mrad. The intersections l_1(Se) and l_2(Sn) give antireflection solutions.

Se and $l_2=39$ Å of Sn to give a multilayer GIAR film with primary minimum at $\phi_0=4.5$ mrad when reflecting 14.4-keV radiation. Figure 12 gives the rocking curve for this case, with the dashed curve at the minimum giving the reflectivity averaged over an angular spread of $\Delta\phi=0.2$ mrad. We note in particular that the angular region of strong suppression is somewhat broader than for the single-layer GIAR films and the first subsidiary maximum is much less pronounced [compare, for example, Fig. 10(a) of paper I], in agreement with the previous qualitative discussion.

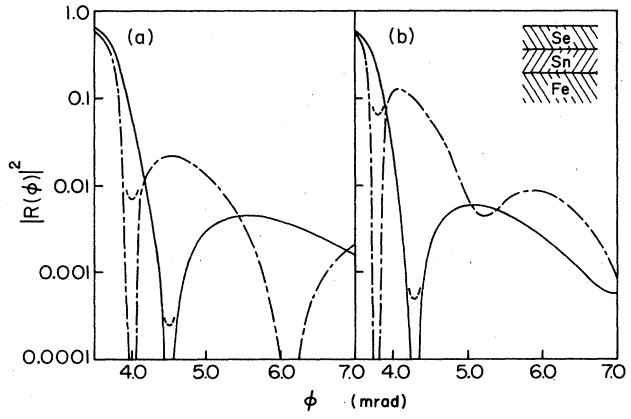

FIG. 12. Rocking curves $|R|^2$ vs ϕ for different coatings l_1(Se) and l_2(Sn) on Fe, determined to give antireflection coats at $\phi_0=4.5$ mrad ($l_1=44$ Å, $l_2=39$ Å), $\phi_0=4.3$ ($l_1=45$ Å, $l_2=51$ Å), $\phi_0=4.0$ ($l_1=39$ Å, $l_2=86$ Å), and $\phi_0=3.8$ ($l_1=19$ Å, $l_2=155$ Å).

Also in Fig. 12, we give the optimum thicknesses l_1(Se) and l_2(Sn) and the 14.4-keV rocking curves for Fe mirrors coated with multilayer GIAR films, with primary minima chosen to occur at $\phi_0=4.3$, 4.0, and 3.8 mrad, respectively. For the last case, $\phi_0<\phi_c$(Fe) and the response is similar to the damping-stabilized films of Sec. III of paper I.

One of the important features of thickness-tuned multilayer GIAR films is that they greatly expand the range of possible materials for producing GIAR films—the only restriction which must be met is Eq. (16). With different choices of materials the response can be quite different.

An example of particular interest is a Fe mirror ($\phi_{c3}=3.84$ mrad) coated with Sn ($\phi_{c2}=3.45$ mrad) and Al ($\phi_{c1}=2.27$ mrad). Figure 13 gives the curves $l_1^{(=)}(l_2)$, $l_1^{\pi}(l_2)$, and $l_1^{3\pi}(l_2)$ for $\phi_0=4.5$ mrad. For the lowest thickness solution, $l_1=47$ Å (Al), $l_2=66$ Å (Sn) and for the second solution, $l_1=66$ Å (Al), $l_2=87$ Å (Sn). Figure 14 gives the rocking curve for the first solution and shows several interesting features: First, the primary minimum is very deep and broad, with an average reflectivity over 0.2 mrad of $\langle |R|^2\rangle \simeq 1.1\times10^{-4}$. Furthermore, the first secondary minimum is now quite close, occurring at 5.6 mrad, the intermediate maximum at 5.0 mrad only peaks to $|R|^2\approx 7.5\times10^{-4}$ and the reflectivity is less than 10^{-3} over the exceptionally broad angular region of 1.7 mrad.

The reason for this behavior can be understood qualitatively from the phasor diagrams given in Fig. 15: Figure

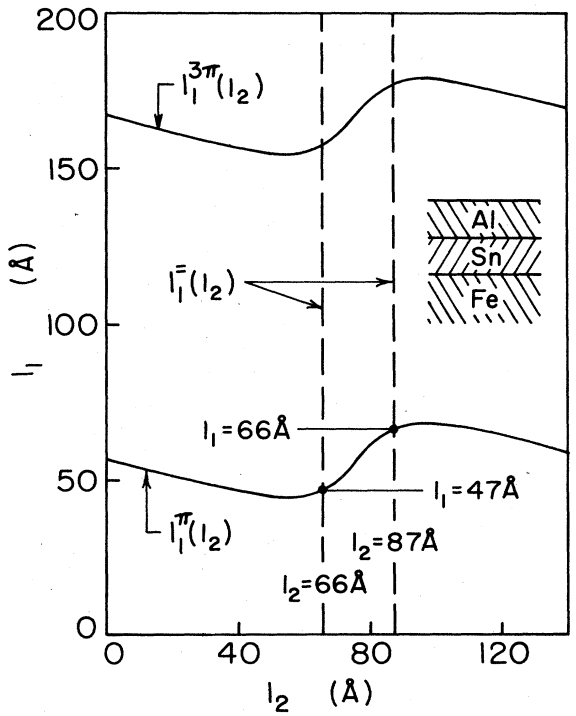

FIG. 13. Graphical solution for l_1(Al) and l_2(Sn) for antireflection coatings on an Fe mirror, reflecting 14.4-keV radiation at $\phi_0=4.5$ mrad.

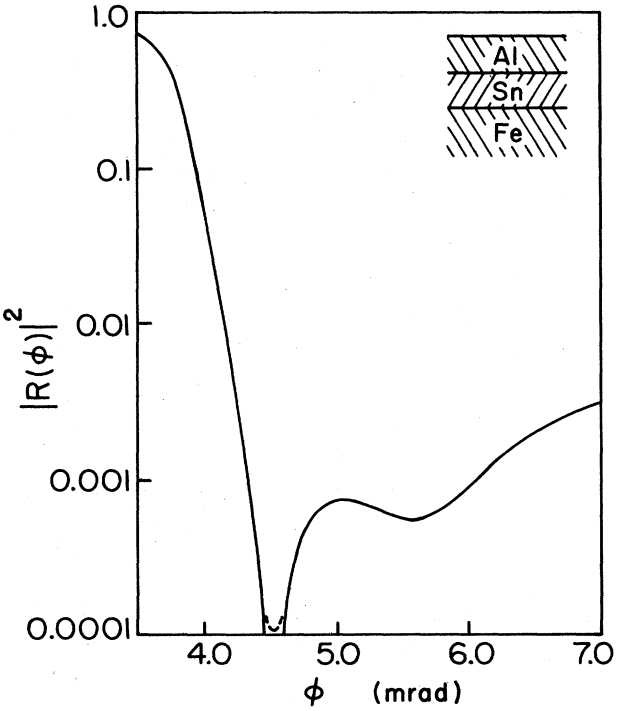

FIG. 14. Rocking curve $|R|^2$ vs ϕ for Fe mirror coated with $l_1=47$ Å (Al), $l_2=66$ Å (Sn), reflecting 14.4-keV radiation.

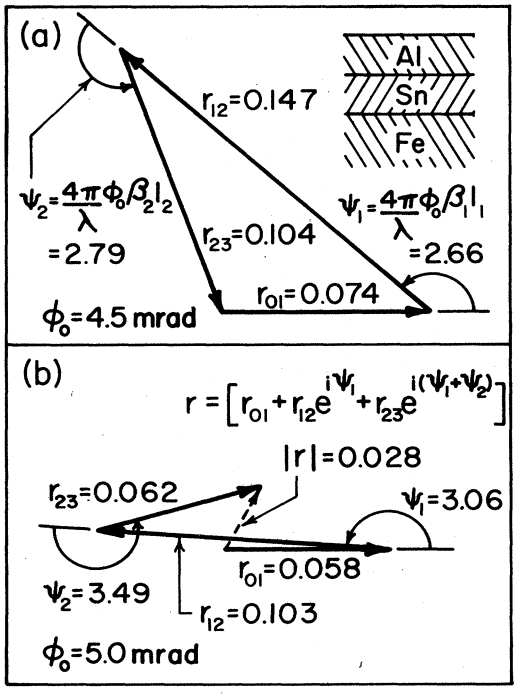

FIG. 15. Phasor-addition diagram for the reflection amplitude R for the mirror of Fig. 14, at (a) the primary minimum $\phi_0=4.5$ mrad, and at (b) the first secondary maximum $\phi=5.0$ mrad.

15(a) gives the phasor diagram at the primary minimum $\phi_0=4.5$ mrad. Because Al is low density while both Sn and Fe have high electron densities, the largest reflection amplitude is r_{12} at the Al-Sn interface and the phasor triangle is strongly "tilted" to the left. Now, as ϕ increases, ψ_1 increases, and the effect is to rotate the tip of the R_{23} phasor downward, which is also the tip of the total R. However, ψ_2 also increases, which tends to rotate the tip back up towards the first quadrant. The combination of these two counteracting rotations, plus the fact that the lengths of the phasor vectors decrease with increasing ϕ, work to keep the resultant R small over an exceptionally large angular region. Figure 15(b) shows the resulting phasor addition diagrams at $\phi=5.0$ (first secondary maximum).

Finally, the two-film formalism can also be applied to give an exact solution for the $3\lambda/8$-coated UT film discussed in the preceding section. We can in fact generalize, letting film 1 and substrate 3 be any two low-density media (but if not identical, the coating will not be a $3\lambda/8$ coating) and we need not require $\phi\simeq\phi_{c2}$. As a particular example, we give the results for an Al-Fe-Si series. Choosing the primary minimum to occur at $\phi_0=\phi_{c2}(\text{Fe})=3.84$ mrad, the optimum thicknesses are $l_1=106$ Å (Al) and $l_2=10$ Å (Fe), while at $\phi_0=4.5$ mrad, $l_1=83$ Å and $l_2=8$ Å. The corresponding rocking curves are shown in Fig. 16.

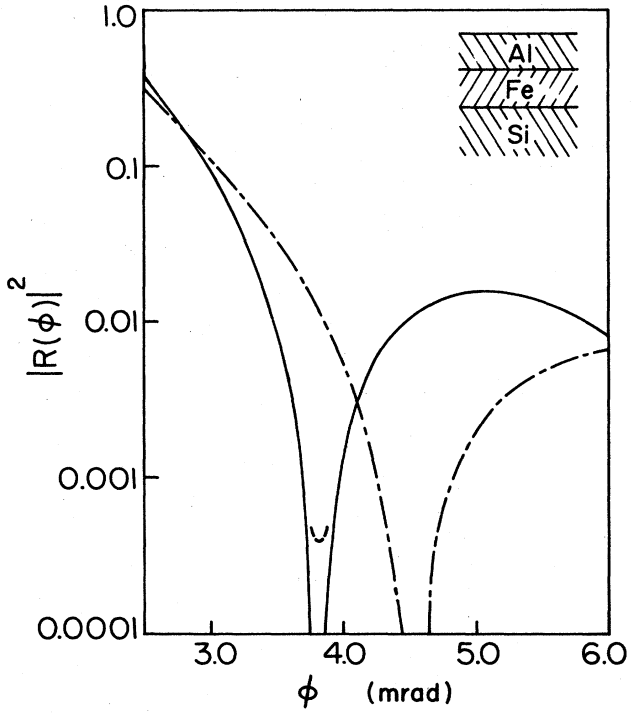

FIG. 16. Rocking curves $|R|^2$ vs ϕ for reflection of 14.4-keV radiation from Si mirrors coated with an ultrathin film l_2(Fe) which is coated with a low-density film l_1(Al). Here, l_1 and l_2 have been determined to give a minimum at $\phi_0=\phi_c$ (Fe)$=3.84$ ($l_1=106$ Å, $l_2=10$ Å) and at $\phi_0=4.5$ mrad ($l_1=83$ Å, $l_2=8$ Å). This is a generalization of a $3\lambda/8$-coated ultrathin film.

2. *Three or more films*

Additional degrees of freedom are introduced by increasing the number of films. For a mirror coated with three films, the necessary condition for there to be antireflection solutions for some choice of l_1, l_2, and l_3 is that

$$r_{ij} < r_{kl} + r_{mn} + r_{pq} \ . \tag{23}$$

However, there will now be a continuum of possible solutions rather than just two. This is easily seen from the graphical construction shown in Fig. 17 for the specific case of an Al(1)-Se(2)-Sn(3) series coated on Fe(4) with $\phi_0 = 4.5$ mrad: the circle C_1 of radius r_{12} is centered at the tip P_1 of the R_{01} vector and the circle C_3 of radius r_{34} is centered at the origin P_0. The circle C_2 of radius r_{23} is centered at P_2, which can be *any point* on C_1. The intersections P_3 and P_3' of C_2 and C_3 determine the two possible solutions for completing the phasor diagram in order that it give exact cancellation. However, since P_2 can be selected arbitrarily on C_1, there is in fact a continuum of possible solutions.

In Fig. 17 we show solutions for two different choices of P_2. From the measured ψ_1, ψ_2, ψ_3, the appropriate film thicknesses are $l_1 = 28$ Å (Al), $l_2 = 19$ Å (Se), and $l_3 = 52$ Å (Sn) (for the solid-line vectors of the diagram) and $l_1 = 14$ Å, $l_2 = 33$ Å, and $l_3 = 44$ Å (for the dashed-line vectors).

The exact treatment is a direct extension of the two-film case: For a mirror coated with three films, the reflection amplitude is

$$R = \frac{R_{01} + R_{12}^{\dagger}(l_2,l_3)e^{i2g_l l_1}}{1 + R_{01}R_{12}^{\dagger}(l_2,l_3)e^{i2g_1 l_1}}$$

$$= \frac{r_{01}e^{i\phi_{01}} + r_{12}^{\dagger}(l_2,l_3)e^{-2g_1'' l_1}e^{i(\phi^{\dagger}(l_2,l_3)+2g_1' l_1)}}{1 + R_{01}R_{12}^{\dagger}e^{i2g_1 l_1}} \ , \tag{24}$$

where now

$$R_{12}^{\dagger}(l_2,l_3) \equiv r_{12}^{\dagger}(l_2,l_3)\exp[i\phi_{12}^{\dagger}(l_2,l_3)]$$

is the compound reflection amplitude for films 2 and 3 plus substrate reflecting into medium 1,

$$R_{12}^{\dagger}(l_2,l_3) = \frac{R_{12} + R_{23}^{\dagger}(l_3)e^{i2g_2 l_2}}{1 + R_{12}R_{23}^{\dagger}(l_3)e^{i2g_2 l_2}} \ , \tag{25}$$

and $R_{23}^{\dagger}(l_3)$ is the compound reflective amplitude for film 3 plus substrate reflecting into medium 2,

$$R_{23}^{\dagger}(l_3) = \frac{R_{23} + R_{34}e^{i2g_3 l_3}}{1 + R_{23}R_{34}e^{i2g_3 l_3}} \ . \tag{26}$$

We now arbitrarily fix *either* l_2 or l_3 in Eq. (24) [consistent with the restriction equation (23)]. The previous analysis then goes through with $r_{12}^{\dagger}(l_2,l_3)$ and $\phi_{12}^{\dagger}(l_2,l_3)$, replacing $r_{12}^{\dagger}(l_2)$ and $\phi_{12}^{\dagger}(l_2)$ in Eqs. (19)—(22). The extension to more than three films is made in the same manner.

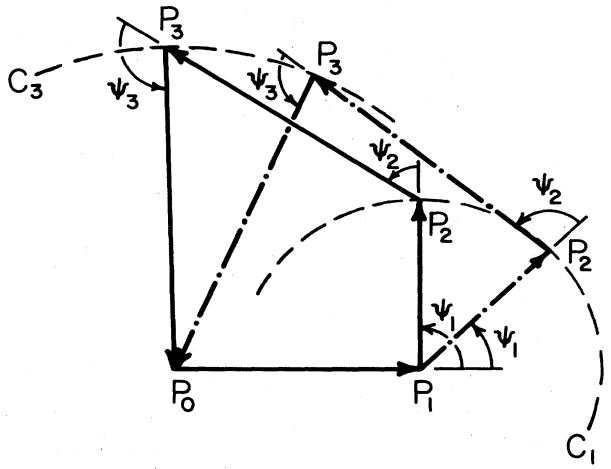

FIG. 17. Graphical solution for l_1(Al), l_2(Se), and l_3(Sn).

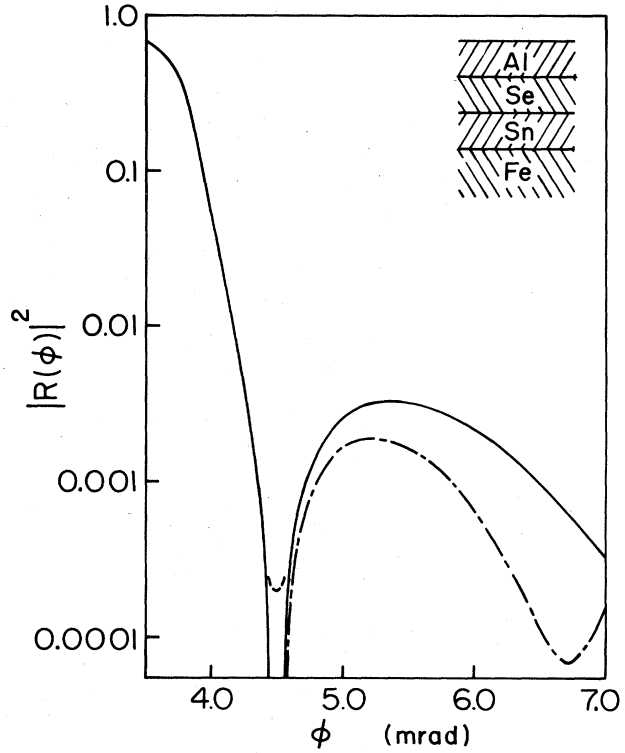

FIG. 18. Rocking curves $|R|^2$ vs ϕ for reflection of 14.4-keV radiation from Fe mirrors coated with l_1(Al), l_2(Se), and l_3(Sn). l_3 is set at (a) 44 Å and (b) 52 Å, and l_1 and l_2 have been determined to give an antireflection minimum at $\phi_0 = 4.5$ mrad. The solid curve is for $l_1 = 20$ Å, $l_2 = 30$ Å, and $l_3 = 44$ Å, and the dashed curve is for $l_1 = 30$ Å, $l_2 = 19$ Å, and $l_3 = 52$ Å.

TABLE I. Optimum thickness l_1(Fe) and l_2(Be) for several choices of l_3(Fe).

l_3(Fe) (Å)	l_1(Fe) (Å)	l_2(Be) (Å)
12	10	60
17	15	57
30	51	26

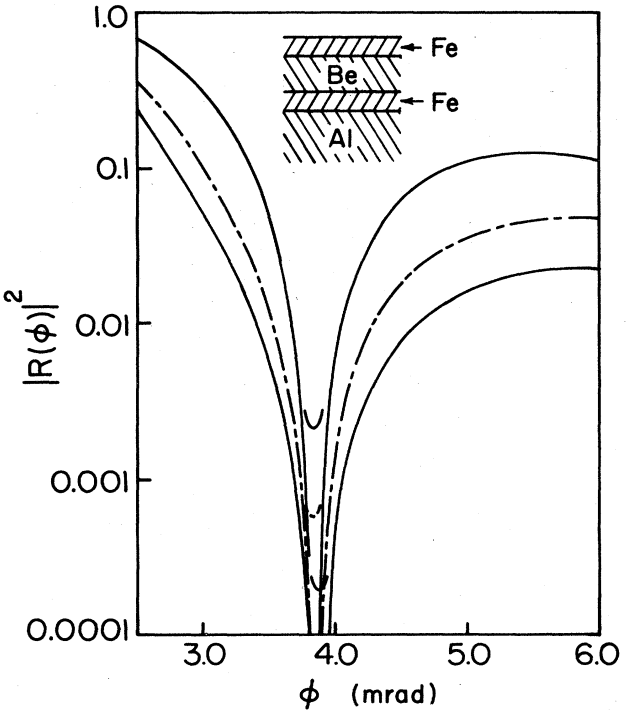

FIG. 19. Rocking curves for layered ultrathin films l_1(Fe), l_2(Be), and l_3(Fe) on Al. Here, l_3(Fe) has been set at (a) 12 Å, (b) 17 Å, and (c) 30 Å, and l_1(Fe) and l_2(Be) have been determined to give the antireflection minimum at $\phi_0=\phi_c$(Fe)=3.84 mrad. For the lower solid curve, $l_1=10$ Å, $l_2=60$ Å, and $l_3=12$ Å; for the dashed curve, $l_1=15$ Å, $l_2=57$ Å, $l_3=17$ Å; and for the upper solid curve, $l_1=26$ Å, $l_2=51$ Å, and $l_3=30$ Å.

For the previous example of Al-Se-Sn coated on Fe, if we choose $\phi_0=4.5$ mrad and set $l_3=52$ Å (Sn), then the optimum thicknesses are $l_1=30$ Å (Al) and $l_2=19$ Å (Se), while if we set $l_3=44$ Å (Sn), then $l_1=20$ Å (Al) and $l_2=30$ Å (Se). In both cases, l_1 and l_2 are shifted from the graphical solutions by the effects of photoabsorption and multiple scattering. Figure 18 shows the rocking curves for the two cases. For either choice of parameters the primary minimum is at $\phi_0=4.5$ mrad, but the locations of the secondary minima vary.

One particular application of the three-film formalism is to give optimum thicknesses l_1,l_2,l_3 for the layered UT-GIAR films discused in the previous section; for example, two UT layers of Fe separated by Be on an Al substrate. Table I gives the optimum thicknesses l_1(Fe), and l_2(Be) for several different choices of l_3(Fe), determined to give the primary minimum at $\phi_0=\phi_{c3}$(Fe)=3.84 mrad. The resulting rocking curves are given in Fig. 19. More generally, the UT films 1 and 3 can be taken as any two high-density materials, media 2 and 4 can be any two low-density materials, and ϕ_0 does not need to be restricted to be equal to ϕ_c.

V. TAPERED IMPEDANCE GIAR FILMS

A limiting case of multilayer GIAR films is the coating of a mirror with a single "tapered" film in which the electron density varies slowly from a very low value to the density of the mirror; e.g., an Fe mirror coated with a carbon-iron film C_xFe_{1-x}, with the carbon fraction $x_1(z)$ slowly decreasing from $1\rightarrow 0$ as $z\propto 0\rightarrow l_1$. If we imagine the film as composed of a large number of strips Δz, there will be a reflection R_{01} from the top surface (vacuum-carbon) and weak reflections,

$$R_{z,z+\Delta z}=\left[\frac{\beta(z)-\beta(z+\Delta z)}{\beta(z)+\beta(z+\Delta z)}\right]\simeq-\frac{d\beta}{dz}\Delta z/2\beta(z)\ , \tag{27}$$

at each interface. The total reflection can be calculated exactly from the multilayer formula, Eq. (12), of paper I or in the single scattering approximation as

$$R\simeq R_{01}+\sum_{z=0}^{l_1}R_{z,z+\Delta z}\exp\left[i\int_0^z 2g(z')dz'\right]\ . \tag{28}$$

The essential point is that by taking a slow gradient, the internal interface reflections are very weak and, if the film is taken sufficiently thick, the internal reflections will also tend to destructively interfere. The total reflection is then dominated by the top surface reflection R_{01} (pure C) which is strongly reduced from a pure Fe reflection R_{02}. The degree of reduction depends on how the electron density is chosen to vary and on the film thickness l_1.

Near-total internal cancellation can be achieved by "λ/N tapering:" For a chosen ϕ_0 take "λ/N increments" $\Delta z=\lambda/[N\phi_0\beta(z)]$ (N large and arbitrary) with the density increasing to give a constant reflection amplitude $R_{z,z+\Delta z}(\phi)=\alpha$ in Eq. (27). The resulting differential equation for $\beta(z)$, with the limits $\beta(z=0)=\beta_1(\phi_0)$, $\beta(z=l_1)=\beta_2(\phi_0)$, determines the required $\beta(z)$ as

$$\beta(z)=\beta_1/[1+(z/l_1)(\beta_1/\beta_2-1)]\ . \tag{29}$$

This also determines the required fractional concentration $x_1(z)$ of carbon, since $\beta(z)=[1-\phi_c^2(z)/\phi_0^2]^{1/2}$, and the critical angle for a two-component mixture is $\phi_c(z)=\{(x_1(z)\phi_{c1}^2+[1-x_1(z)]\phi_{c2}^2\}^{1/2}$. With this choice of density variation, the total reflectivity at ϕ_0 becomes (in the single scattering approximation)

$$R(\phi_0)\simeq R_{01}-i\alpha'(e^{i2k\phi_0\bar{\beta}l_1}-1)\ , \tag{30}$$

with

$$\bar{\beta}=[\beta_2\beta_1/(\beta_1-\beta_2)]\ln(\beta_1/\beta_2)$$

and

$$\alpha'=[\ln(\beta_1/\beta_2)/4k\phi_0\bar{\beta}l_1]\ .$$

By tapering over a sufficiently large thickness l_1, then, $\alpha'\lesssim R_{01}(\ll R_{02})$ and the top surface reflection dominates. For C_xFe_{1-x} with $\phi_0=4.3$ mrad, this requires $l_1\gtrsim 300$ Å. However, it is also possible to achieve near-total destructive interference of the internal reflections by taking $l_1\simeq n(\lambda/2\phi_0\bar{\beta})$, which for the C_xFe_{1-x} example requires $l_1\simeq n(160$ Å).

Figure 20 shows the rocking curves, calculated from Eq. (12) of paper I using $\Delta z=20$ Å strips, for an Fe mirror coated with a tapered C_xFe_{1-x} film, with the density

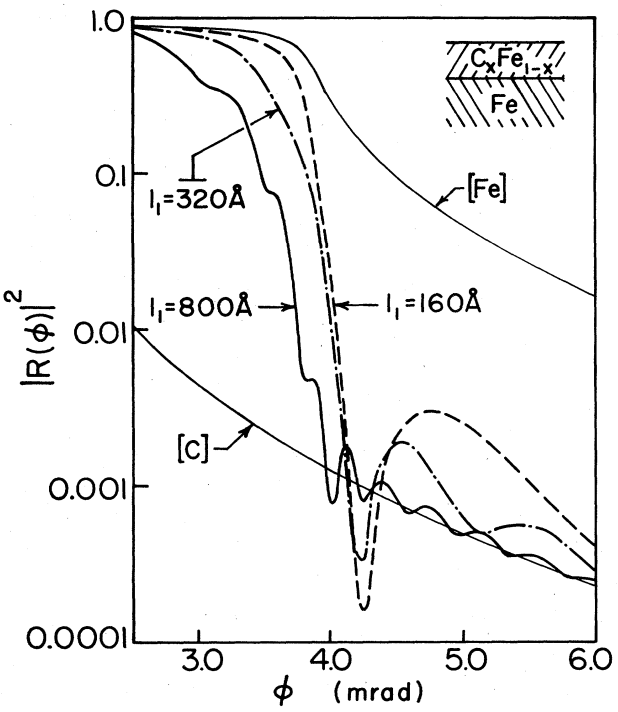

FIG. 20. Rocking curves for Fe mirror coated with tapered C_xFe_{1-x} film, with density variation $x(z)$ taken to produce a λ/N-tapered film at $\phi_0=4.3$ mrad for $l_1=160$, 320, and 800 Å.

variation taken to produce a λ/N-tapered film at $\phi_0=4.3$ mrad for $l_1=160$, 320, and 800 Å. The reflectivities $|R_{01}|^2$ and $|R_{02}|^2$ for pure C and Fe are also given for comparison. The interference minimum is slightly shifted from ϕ_0 and, more importantly, there is a partial cancellation of the upper surface reflection so that the reduction is even stronger than anticipated by the single scattering approximation equation (30). Even away from ϕ_0, where there are no exact phase cancellations, the reflectivity is still strongly reduced by the tapering, and for large angles approaches $|R_{01}|^2$.

The main advantage of such a tapered GIAR film is that it gives a strong suppression over a very broad angular range and, correspondingly, over a broad frequency range. The obvious disadvantage is the control problem of fabricating a film with the proper density variations. There are other equally good tapering schemes, and even stronger cancellation of the upper surface reflection should be possible.

VI. SUMMARY

The purpose of this paper has been to examine more general techniques for producing grazing-incidence antireflection films to suppress the reflection of 1 Å x rays. Our main conclusions follow.

If a mirror is coated with a film of *higher* electron density, no antireflection films are possible; however, the reflectivity can still be reduced ($\approx\frac{1}{5}$ times) by using a *half-wave film* interference minimum. Although the intensity reduction is much less pronounced than for a $\lambda/4$-GIAR film, a $\lambda/2$ film has the advantage that interference minima will occur for any chosen l_1, and ϕ_0 can be chosen by varying l_1.

Reflectivities can also be reduced by taking a *single ultrathin film* on a low-density backing. For example, with 10-Å Fe on Be the reflectivity is only $\approx 1\%$ in a region where a pure Fe mirror has a 30% reflectivity. A true GIAR film is possible by using *two layered UT films* separated by a low-density $\lambda/4$ film. Because all contributing reflection amplitudes are small, a very deep interference minimum should be possible even without exact impedance matching.

The greatest versatility is offered by *multilayer techniques*. By going to multilayer coatings, the choice of possible materials for GIAR films is greatly extended, and by "thickness tuning," it is possible to arbitrarily specify the operating angle ϕ_0. Furthermore, with an appropriate choice of materials, it is possible to greatly broaden the angular and frequency regions of strong suppression.

A limiting case of multilayer films is a *tapered GIAR film*. Here the combined effects of a slow gradient increase of electron density and destructive interference give a strongly reduced reflectivity—essentially just that of the upper low-density interface. Such films may be of limited practical use, but they are useful for understanding the effects of surface and volume roughness, which we examine in a following paper.[5]

ACKNOWLEDGMENTS

This work was partially supported by the National Science Foundation, Grant No. DMR-80-15706, and the Deutsche Forschungsgemeinschaft and the Bundesministerium für Forschung und Technologie, Grant No. 05269GU.

[1]J. P. Hannon *et al.*, preceding paper, Phys. Rev. B 32, 5068 (1985), henceforth referred to as paper I.

[2]H. A. Macleod, *Thin Film Optical Filters* (Elsevier, New York, 1969), and references therein.

[3]A. Vasicek, *Optics of Thin Films* (North-Holland, Amsterdam, 1960).

[4]M. Bron and E. Wolf, *Principles of Optics* (Pergamon, New York, 1959), pp. 50—69.

[5]J. P. Hannon, J. T. Hutton, G. T. Trammell, E. Gerdau, and R. Rüffer, paper VI (unpublished).